

## Supporting Information

One-step freezing temperature crystallization of layered rare-earth hydroxide ( $\text{Ln}_2(\text{OH})_5\text{NO}_3 \cdot n\text{H}_2\text{O}$ ) nanosheets for a wide spectrum of Ln (Ln=Pr-Er, and Y), anion exchange with fluorine and sulfate, and microscopic coordination probed via photoluminescence

Xiaoli Wu,<sup>a,b,c</sup> Ji-Guang Li,<sup>\*ab</sup> Qi Zhu,<sup>a</sup> Weigang Liu,<sup>a</sup> Jing Li,<sup>ab</sup> Xiaodong Li,<sup>a</sup>

Xudong Sun,<sup>a</sup> and Yoshio Sakka<sup>b</sup>

<sup>a</sup>*Key Laboratory for Anisotropy and Texture of Materials (Ministry of Education) and School of Materials and Metallurgy, Northeastern University, Shenyang, Liaoning 110819, China*

<sup>b</sup>*Advanced Materials Processing Unit, National Institute for Materials Science, Namiki 1-1, Tsukuba, Ibaraki 305-0044, Japan*

<sup>c</sup>*College of Materials Science and Engineering, Guilin University of Technology, Guilin, Guangxi 541004, China*

\*Corresponding author

Dr. Ji-Guang Li

National Institute for Materials Science

E-mail: [LI.Jiguang@nims.go.jp](mailto:LI.Jiguang@nims.go.jp)

Tel: +81-29-860-4394

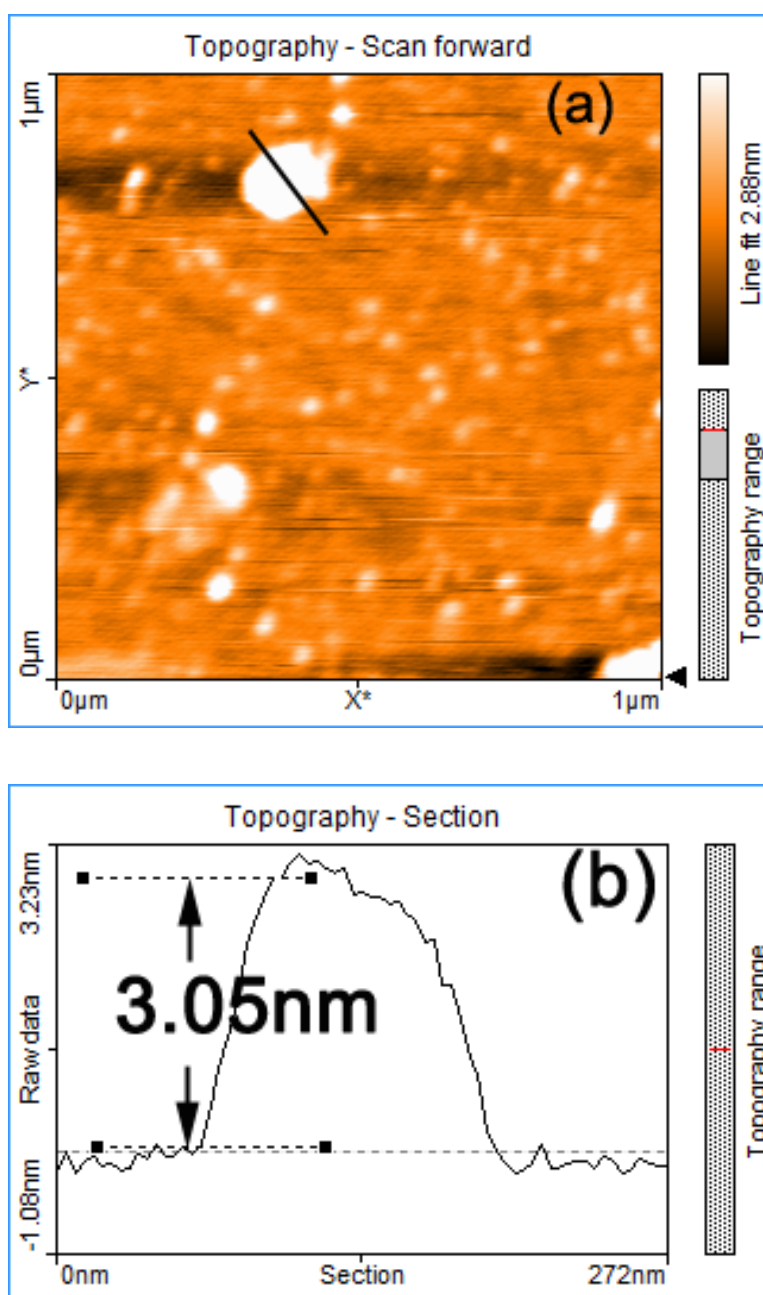


**Figure S1.** AFM observation of the  $Y_2(OH)_5NO_3 \cdot nH_2O$  LRH nanosheets, with (a) the scan mode and (b) height profile analysis of the marked object. The very thin nature and limited lateral size of the nanosheets make clearer imaging rather challenging.

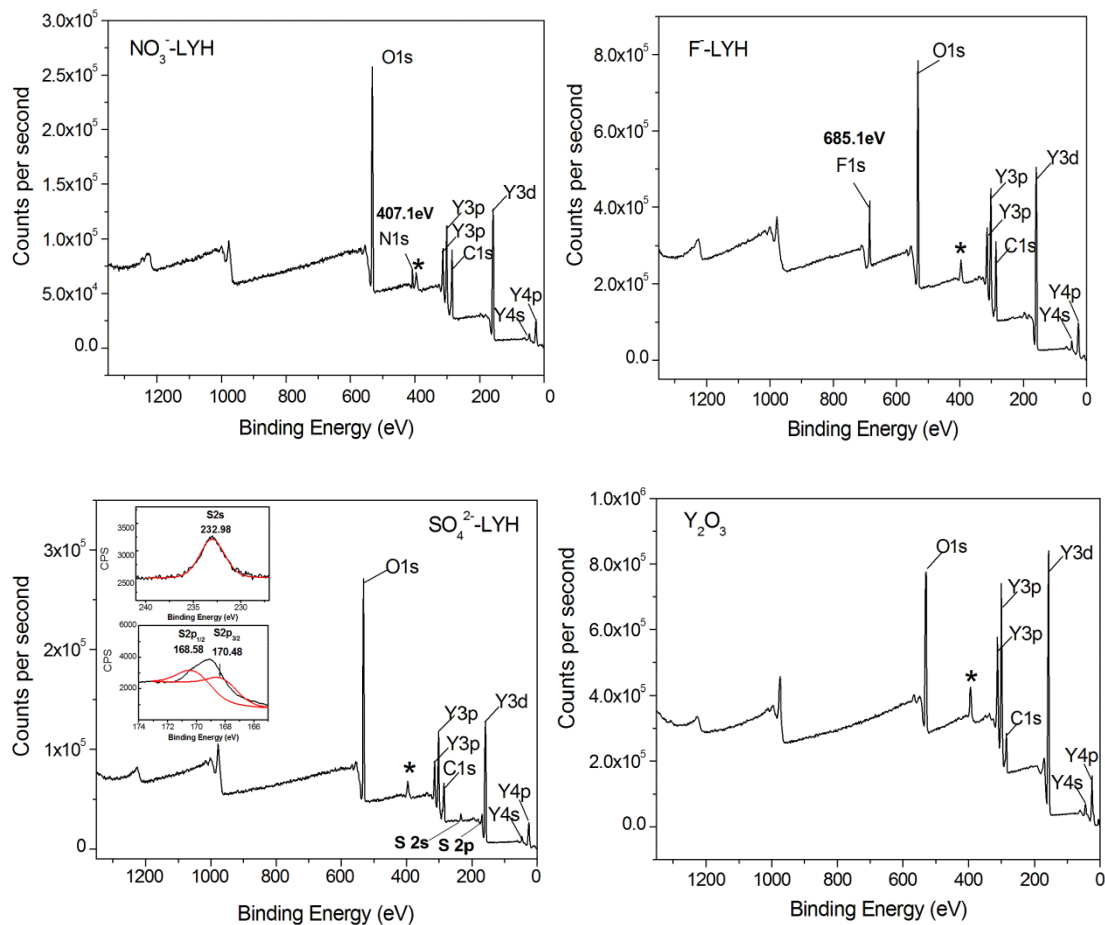


**Figure S2.** XPS survey spectra for the pristine LYH ( $\text{NO}_3^-$ -LYH) and the products anion exchanged with  $\text{F}^-$  ( $\text{F}^-$ -LYH) and  $\text{SO}_4^{2-}$  ( $\text{SO}_4^{2-}$ -LYH). The peak ( $\sim 396$  eV) indicated with an asterisk is also for N-1s, but possibly comes from nitride contamination of the equipment or protective  $\text{N}_2$  gas since it is similarly found for an high purity  $\text{Y}_2\text{O}_3$  powder (99.99%, Kanto Pure Chemicals, Tokyo, Japan). The XPS results indicate that anion exchange of the interlayer  $\text{NO}_3^-$  is essentially complete, as evidenced by the disappearance of the N-1s signal as in nitrate at 407.1 eV and the emergence of the F-1s signal at 685.1 eV and the S-2s ( $\sim 233$  eV) and S-2p ( $\sim 165$ -173 eV) signals.

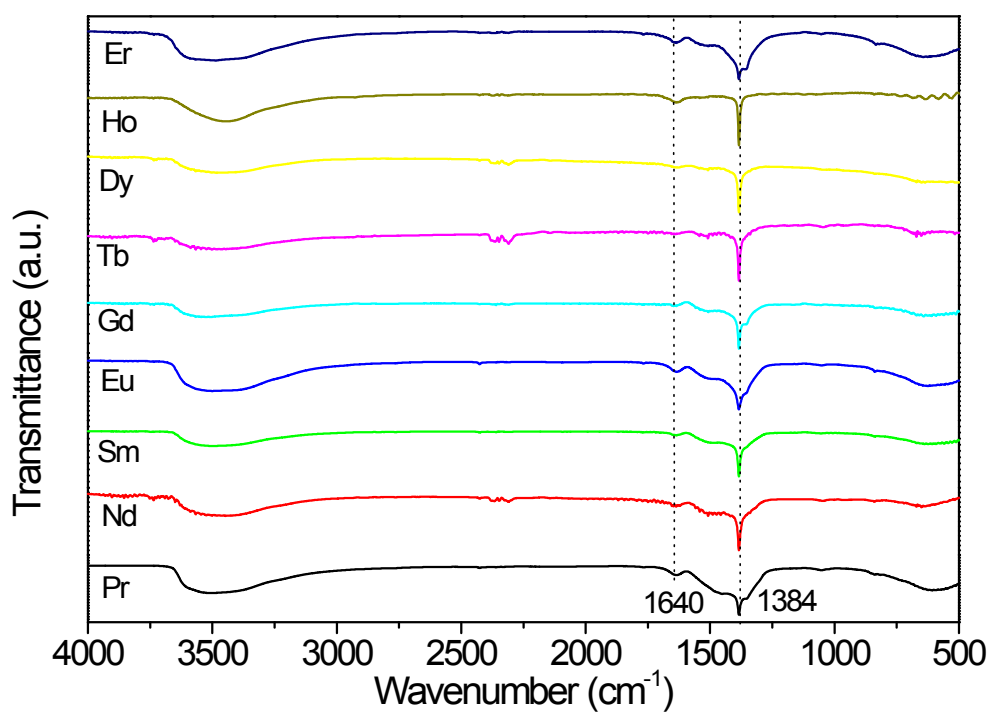


**Figure S3.** FT-IR spectra of the  $\text{Ln}_2(\text{OH})_5\text{NO}_3 \cdot n\text{H}_2\text{O}$  nanosheets crystallized at  $\sim 4^\circ\text{C}$ , with the type of Ln indicated.

**Table S1.** Results of chemical analysis for  $\text{Ln}_2(\text{OH})_5\text{NO}_3 \cdot n\text{H}_2\text{O}$  and the derived chemical formula. Carbon was assumed to solely come from  $\text{CO}_3^{2-}$  and  $\text{CO}_3^{2-}$  was assumed to replace  $\text{OH}^-$ . The amount of  $\text{OH}^-$  was derived from molecular neutrality.

	Chemical analysis (wt%)			Chemical formula
	Ln	$\text{NO}_3^-$	C	
Pr	62	13.7	0.37	$\text{Pr}_2(\text{OH})_{4.72}(\text{NO}_3)_{1.0}(\text{CO}_3)_{0.14} \cdot 1.23\text{H}_2\text{O}$
Nd	62.8	13.5	0.37	$\text{Nd}_2(\text{OH})_{4.74}(\text{NO}_3)_{0.98}(\text{CO}_3)_{0.14} \cdot 1.17\text{H}_2\text{O}$
Sm	63.7	13.1	0.35	$\text{Sm}_2(\text{OH})_{4.74}(\text{NO}_3)_{0.98}(\text{CO}_3)_{0.14} \cdot 1.20\text{H}_2\text{O}$
Eu	64	13.1	0.35	$\text{Eu}_2(\text{OH})_{4.74}(\text{NO}_3)_{0.98}(\text{CO}_3)_{0.14} \cdot 1.18\text{H}_2\text{O}$
Gd	64.8	12.8	0.35	$\text{Gd}_2(\text{OH})_{4.72}(\text{NO}_3)_{1.0}(\text{CO}_3)_{0.14} \cdot 1.12\text{H}_2\text{O}$
Tb	65	12.7	0.34	$\text{Tb}_2(\text{OH})_{4.72}(\text{NO}_3)_{1.0}(\text{CO}_3)_{0.14} \cdot 1.14\text{H}_2\text{O}$
Dy	65.5	12.5	0.34	$\text{Dy}_2(\text{OH})_{4.54}(\text{NO}_3)_{1.0}(\text{CO}_3)_{0.14} \cdot 1.31\text{H}_2\text{O}$
Ho	66	12.4	0.28	$\text{Ho}_2(\text{OH})_{4.76}(\text{NO}_3)_{1.0}(\text{CO}_3)_{0.12} \cdot 1.10\text{H}_2\text{O}$
Er	66	12.3	0.28	$\text{Er}_2(\text{OH})_{4.74}(\text{NO}_3)_{1.02}(\text{CO}_3)_{0.12} \cdot 1.18\text{H}_2\text{O}$
Y	51	17.8	0.48	$\text{Y}_2(\text{OH})_{4.72}(\text{NO}_3)_{1.0}(\text{CO}_3)_{0.14} \cdot 1.12\text{H}_2\text{O}$

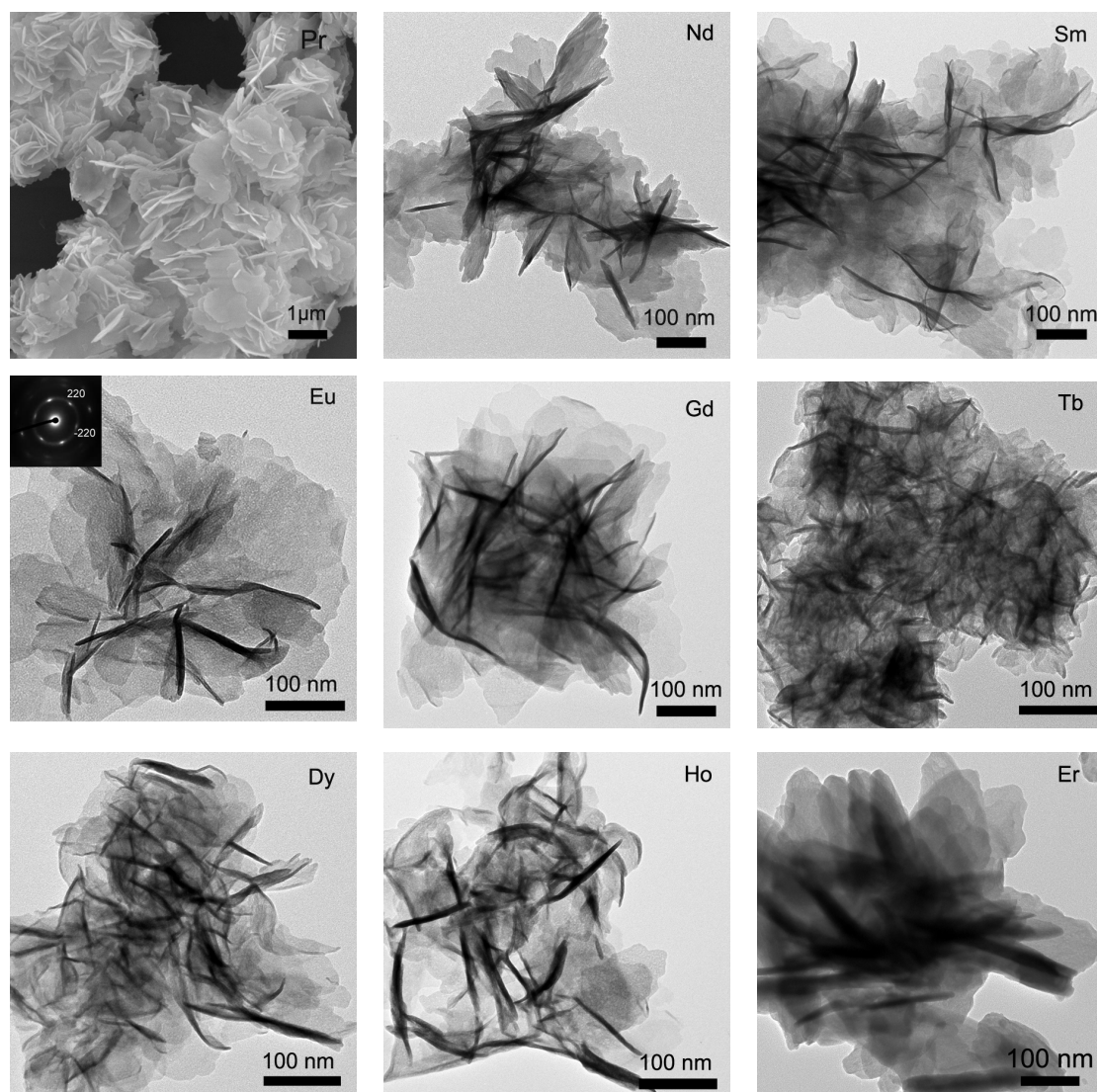


**Figure S4.** FE-SEM (for Pr) and TEM (for the rest) morphologies of the  $\text{Ln}_2(\text{OH})_5\text{NO}_3 \cdot n\text{H}_2\text{O}$  nanosheets.

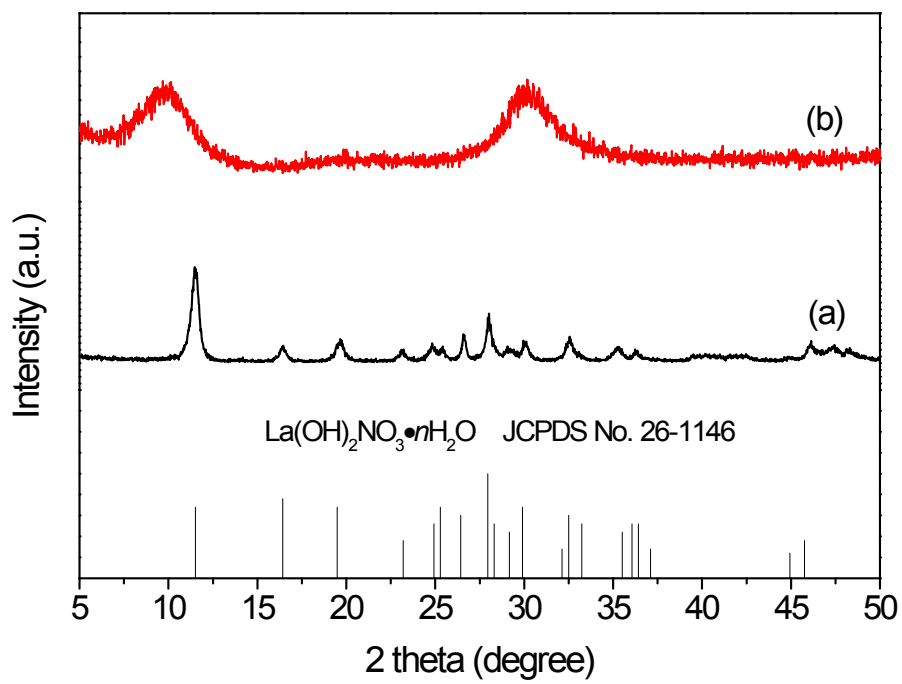


**Figure S5.** XRD patterns of the products precipitated at 4 °C for La (a) and Tm (b).

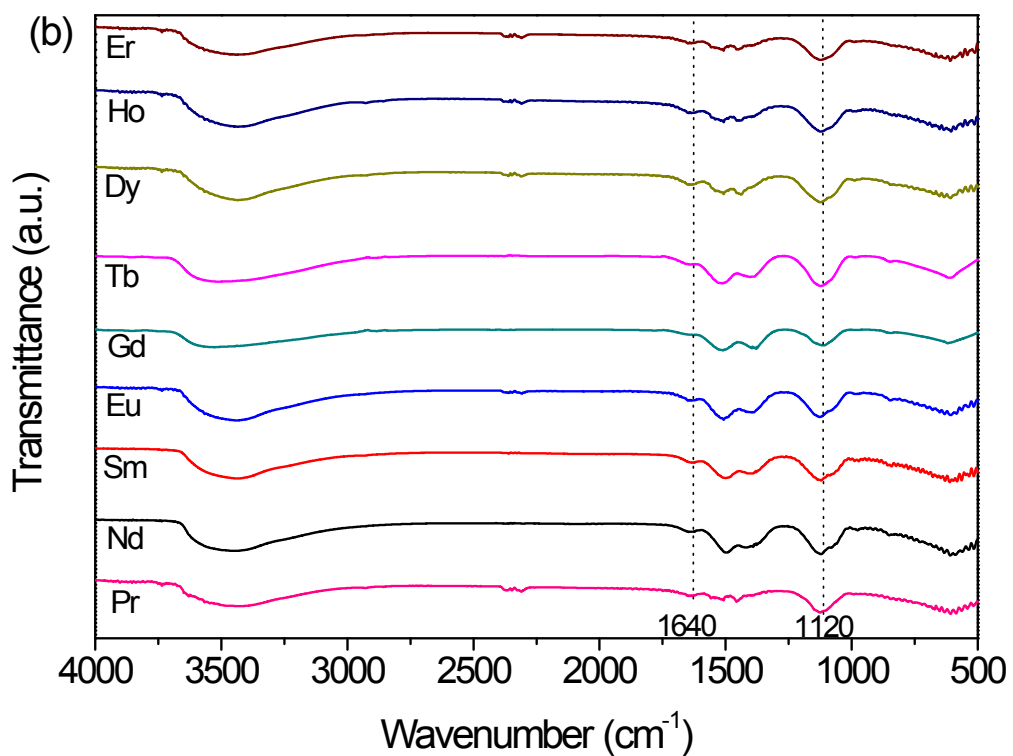
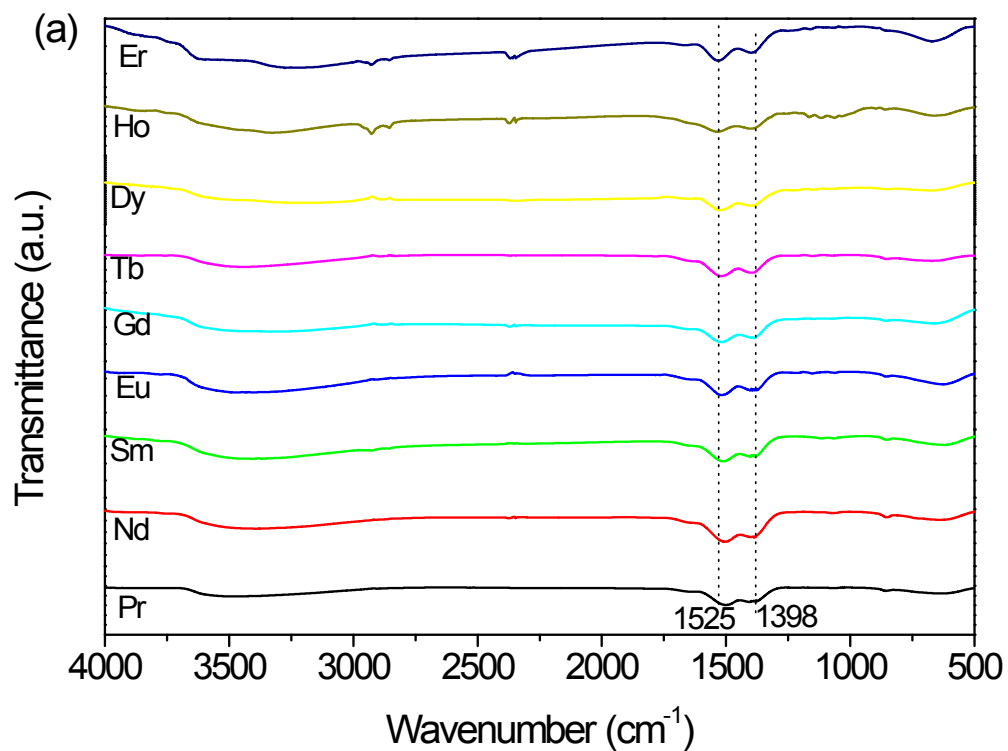


**Figure S6.** FT-IR spectra of the products obtained via anion exchange of  $\text{Ln}_2(\text{OH})_5\text{NO}_3 \cdot n\text{H}_2\text{O}$  with  $\text{F}^-$  (a) and  $\text{SO}_4^{2-}$  (b).



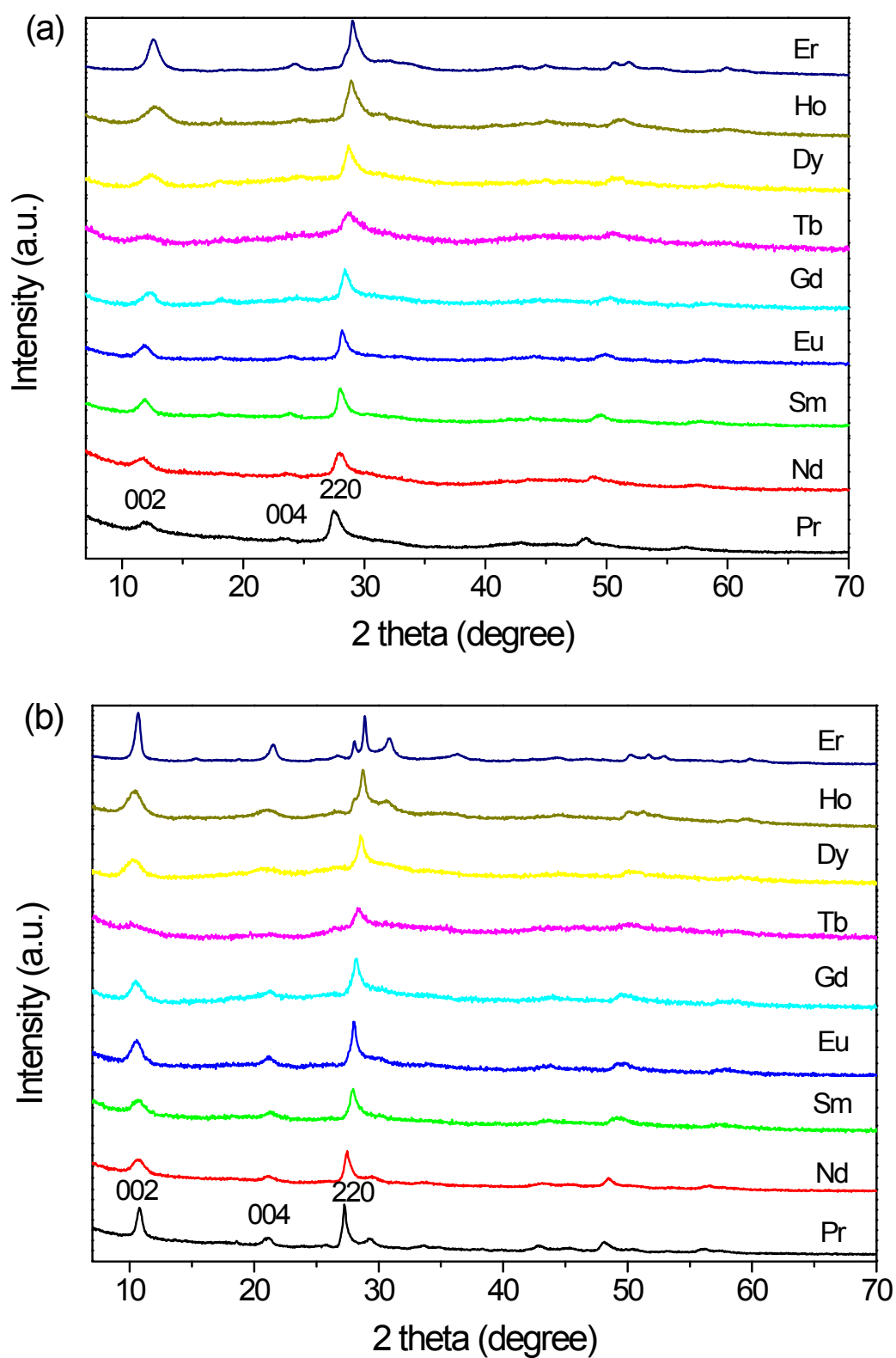


**Figure S7.** Powder XRD patterns for the products obtained via anion exchange of  $\text{Ln}_2(\text{OH})_5\text{NO}_3 \cdot n\text{H}_2\text{O}$  with  $\text{F}^-$  (a) and  $\text{SO}_4^{2-}$  (b).